scientific data

OPEN

DATA DESCRIPTOR

Dataset of tensile properties for sub-sized specimens of nuclear structural materials

Longze Li[1], John W. Merickel[2], Yalei Tang[2], Rongjie Song[2], Joshua E. Rittenhouse[2], Aleksandar Vakanski[1] ✉ & Fei Xu[2] ✉

Mechanical testing with sub-sized specimens plays an important role in the nuclear industry, facilitating tests in confined experimental spaces with lower irradiation levels and accelerating the qualification of new materials. The reduced size of specimens results in different material behavior at the microscale, mesoscale, and macroscale, in comparison to standard-sized specimens, which is referred to as the "specimen size effect." Although analytical models have been proposed to correlate the properties of sub-sized specimens to standard-sized specimens, these models lack broad applicability across different materials and testing conditions. The objective of this study is to create the first large public dataset of tensile properties for sub-sized specimens used in nuclear structural materials. We performed an extensive literature review of relevant publications and extracted over 1,000 tensile testing records comprising 55 columns including material type and composition, manufacturing information, irradiation conditions, specimen dimensions, and tensile properties. The dataset can serve as a valuable resource to investigate the specimen size effect and develop computational methods to correlate the tensile properties of sub-sized specimens.

Background & Summary

The development of advanced nuclear reactor concepts aims to enhance the safety, economics, waste management, and non-proliferation security of commercial nuclear power reactors[1]. The advanced reactor designs typically operate under more extreme conditions with higher temperatures and increased radiation levels compared to current light water reactors[2,3]. Such conditions necessitate the timely development of suitable advanced materials and processes. Unlike materials development in other sectors which typically spans a few years[4], the development and qualification of nuclear materials are prolonged due to the need for extensive testing and experiments to assess in-reactor performance. Accelerated irradiation testing thus is crucial for rapidly achieving high irradiation doses and understanding the behavior and irradiation responses of new materials[5].

Small-scale mechanical testing with sub-sized specimens in the nuclear industry enables faster irradiation tests and reduces the time for deployment of new materials[5–7]. Importantly, small-scale mechanical testing allows for greater utility of constrained experimental spaces within nuclear test facilities, and enables researchers to conduct a greater number of experiments while simultaneously reducing the radiological dose emitted by irradiated materials, which is directly proportional to their volume[8,9].

Despite the advantages of mechanical testing with sub-sized specimens, this approach is marked with several challenges, such as the demand for enhanced testing precision and advanced measurement methods, sensitivity to testing conditions and dimensional deviations, as well as increased impact of the sample preparation, processing techniques, and surface defects on the test results. Consequently, mechanical properties of sub-sized specimen materials are often reported to exhibit greater variability compared to standard-sized specimens[9–11]. The varying material behavior due to the reduced dimensions of sub-size specimens in comparison to standard-sized specimens is commonly referred to as the specimen size effect or scaling effect[5,6,12–14]. In general, this effect encompasses a broad range of other factors impacting measured material properties beyond specimen size and geometry, and involves microstructural changes and inhomogeneity, surface effects, and anisotropy resulting from the differences in the microstructure and crystallographic texture[10]. Failing to account for the specimen

[1]Department of Computer Science, University of Idaho, Moscow, ID, USA. [2]Idaho National Laboratory, Idaho Falls, ID, USA. ✉e-mail: vakanski@uidaho.edu; Fei.Xu@inl.gov

size effect can lead to incorrect estimates of material properties and load-bearing capabilities, which can potentially result in catastrophic consequences in critical applications, such as the nuclear industry.

Extensive research has been conducted to develop models that link the test results from sub-sized specimens to those of standard-sized specimens[5–15]. Techniques for conversion of elongation based on the Bertella-Oliver formula[14] or Barba's law[15] have been broadly adopted for correcting the measurements of small-size specimens, provided that the bulk material properties are maintained. The inverse Finite Element Method (FEM) has also been utilized to predict true stress-strain relationships from engineering strain-stress curves based on minimizing the deviations in contact-type strain measurements[16,17]. The FEM method is also used for predicting the material behavior beyond the yield point and after necking[18]. Additionally, several application standards provide recommendations on conversion methods for the mechanical properties of sub-sized specimens and standard-sized specimens[19]. On the other hand, existing analytical models and conversion methods are typically developed for specific materials and tests and/or introduce certain assumptions that limit their applicability across different testing conditions and materials. Consequently, these models may produce inaccurate results under varying conditions and for different materials[20]. Furthermore, many analytical models do not provide means to evaluate the importance of test conditions or individual input features on the specimen size effect.

Recent progress in Machine Learning (ML) offers unique potential to advance materials science[21–23], due to the capacity for modelling complex combinatorial spaces of multi-physics and multi-scale mechanisms, which traditional analytical methods are unable to resolve or can only address at a significant computational expense. These ML advantages can be effective in addressing the challenges related to specimen size effect in mechanical tests[24,25]. Despite the promising capabilities, a major obstacle that hinders the wide application of ML-based approaches in materials science is the lack of large, curated datasets with well-organized and consolidated information for various materials and testing conditions. The scattered nature of helpful information in the published literature on mechanical tests and other material information prevents the direct application of data-driven ML methods.

The objective of this study is to systematically gather reliable data for investigating the specimen size effect on the tensile properties of nuclear structural materials. The focus is on studying the influence of specimen dimensions and geometry on mechanical properties such as yield strength, ultimate tensile strength, uniform elongation, and total elongation. The dataset was created through an extensive literature review of scientific articles and databases. The search inclusion criteria targeted peer-reviewed studies on tensile testing of sub-sized specimens, providing quantitative data on tensile properties relative to specimen size. The extracted data points from the literature review were organized into a tabular format database containing 1,050 tensile testing records with 55 columns, including material type and composition, manufacturing information, irradiation conditions, specimen size and dimensions, and tensile properties. Materials science experts conducted systematic checks to validate the collected data, ensuring accuracy in the material type, manufacturing processes and treatment methods, and testing conditions, as well as verifying the chemical composition and other pertinent information. Our team performed statistical analyses to identify and address data outliers, ensuring the reliability of the dataset.

The contributions of this work are as follows:

- Presents the first large curated public dataset of tensile properties for sub-sized specimens of three common groups of nuclear structural materials.
- Involves a comprehensive literature review to collect over 1,000 data records of tensile tests encompassing 55 columns, related to material type and composition, manufacturing information, irradiation conditions, specimen size and dimensions, and tensile properties.
- Provides a valuable resource readily available to researchers and engineers for developing computational and ML-based methods for establishing correlations between the tensile properties of sub-sized and standard-sized specimens.

Methods

Sub-sized specimens are also referred to as small-size, small-scale, mini-size, or miniaturized specimens in various studies[7,26]. Sub-sized specimens were initially developed in the 1970s for testing materials for nuclear reactors due to limited space for experiments in neutron facilities[27,28]. In addition, smaller specimen volumes reduce induced activation, thereby reducing environmental pollution. There has been an increasing demand for using sub-sized specimens in other domains and industries where a limited amount of material is available, such as for assessing the residual life of in-service components by scooping out a small volume of material. Other related applications include evaluating the mechanical properties of micro-electromechanical systems, additively manufactured parts, in rapid alloy prototyping, for measuring local properties in welded parts, and other similar uses[29–32].

Miniaturized Tensile Test (MTT) is a technique for evaluating the tensile properties of materials using sub-sized specimens with the smallest dimension ranging from hundreds of microns to several millimeters[7,33]. MTT is a result of a sustained research and engineering effort based on international collaborations toward standardizing tensile testing with sub-sized specimens. MTT faces various challenges that stem from the specimen size effect, requirements for specialized high-precision equipment and testing procedures, and increased sensitivity to dimensional deviations, specimen fabrication and preparation, surface defects, and other factors. Although numerous studies have been dedicated to addressing the challenges and improving the reliability of MTT, it remains an open topic of research. The following sections present a brief overview of tensile testing and discuss the related challenges of the specimen size effect and design of sub-sized specimens for MTT.

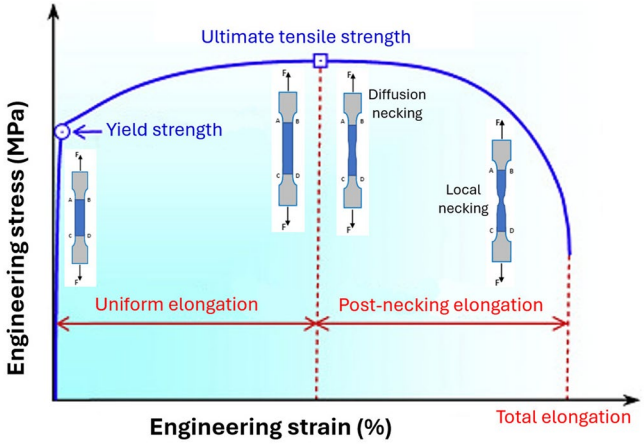

Fig. 1 Engineering stress-strain curve in tensile test.

Tensile test basics. Tensile test is a mechanical test in which a specimen of material undergoes controlled tension until it fractures. The specimen is typically shaped as a cylindrical profile with a uniform cross-sectional area in the middle (also known as dog-bone shape) to ensure uniform distribution of force and predictable failure locations. The specimen is placed in a tensile testing machine that clamps each end, and longitudinal pulling force is applied stretching the specimen at a consistent rate until it fractures[15].

The main outcome of a tensile test is the engineering stress-strain curve shown in Fig. 1, which illustrates the material behavior as the load is applied. The stress value σ is derived by dividing the applied axial force F with the original cross-sectional area A_0 of the specimen.

$$\sigma = \frac{F}{A_0} \tag{1}$$

The engineering strain e is unitless, and it is computed using Eq. (2), where L_i represents the instantaneous length and L_0 is the initial length of the specimen before the test starts.

$$e = \frac{L_i - L_0}{L_0} \tag{2}$$

The engineering stress-strain curve provides important information about the mechanical properties of a material. *Yield strength* (YS) σ_s is defined as the maximum stress that a material can withstand before it begins to deform plastically. When the applied stress is less than σ_s, the material will recover its original shape once the applied force is removed. *Ultimate tensile strength* (UTS) σ_u, also referred to as tensile strength, is the highest stress that a material can endure while being stretched until it breaks, and it corresponds to the peak stress on the stress-strain curve just before the material fails and fractures. Once the material reaches UTS, it has achieved the peak capacity to handle stress and starts to neck, where necking refers to the drastic local plastic deformation. *Uniform elongation* (UE) e_u is the maximum elongation the material can achieve before necking happens. *Total elongation* (TE) e_f is also known as fracture elongation or total elongation at fracture, and it represents the sum of the uniform elongation e_u and *post-necking elongation* (PE) e_p.

$$e_f = e_u + e_p \tag{3}$$

While engineering stress-strain curves are generally used in assessing the tensile mechanical properties of materials, true stress-strain curves more accurately reflect the constitutive behavior of materials and are typically used for theoretical analysis, high precision applications, and detailed mechanical calculations. The true stress σ_t is calculated as the applied load F divided by the instantaneous cross-sectional area A_i of the sample.

$$\sigma_t = \frac{F}{A_i} \tag{4}$$

The true strain e_t is calculated as the natural logarithm of the instantaneous length L_i divided by the original length L_0.

$$e_t = \ln\left(\frac{L_i}{L_0}\right) \tag{5}$$

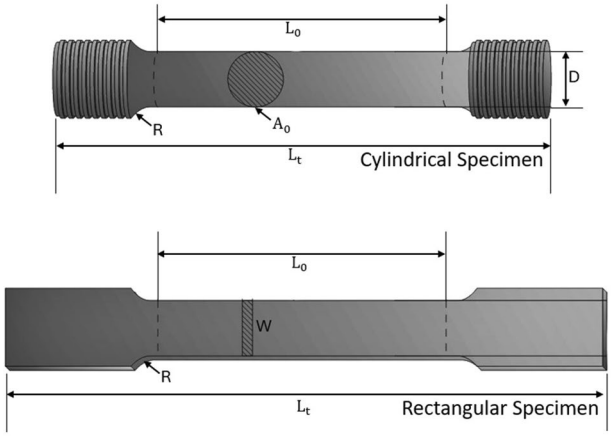

Fig. 2 Tensile specimen examples with cylindrical (round) and rectangular (flat) shape. L_0 is gauge length, L_t is total length, and R is the radius of the fillet. A_0 denotes the cross-sectional area for the cylindrical specimen and W denotes the width for the flat specimen.

Specimen size effect. As stated before, the *specimen size effect* refers to the difference in the measured mechanical properties for specimens with reduced dimensions in comparison to standard-sized specimens. As the specimen size is reduced beyond a certain threshold, correlating the properties of sub-sized specimens with those of standard-sized specimens using analytical methods becomes challenging. The challenges arise not only from the inconsistencies in scaling the material microstructure relative to the changes in material properties at the mesoscale and macroscale, but also from the differences in the specimen geometry at the microscale due to the impact of residual stresses and surface roughness.

Two main design types of sub-sized specimens include flat (rectangular) specimens and round (cylindrical) specimens, as depicted in Fig. 2.

In flat sub-sized specimens, strength and ductility are affected when the specimen thickness is reduced below a certain value. Specifically, the thickness impacts yield strength, ultimate tensile strength, uniform elongation, post-necking elongation, and total elongation. The critical thickness largely depends on the thickness-to-grain size ratio T/GS, and for most materials the critical value of the ratio is between 6 and 10[34,35]. Particularly, when the T/GS is below the critical value, the increase in surface layer grains causes increased dislocation density that cannot maintain the strain hardening rate of the bulk material, and results in decreased flow stress and uniform elongation. When the T/GS ratio is above the critical value, strength and ductility remain nearly constant.

Specimen width also influences the test results for ultimate tensile strength, post-necking elongation, and total elongation in flat sub-sized specimens, even when the thickness is sufficient to represent bulk material properties. A critical width value is typically determined based on the width-to-thickness ratio W/T being approximately 5. When W/T is above 5, ultimate tensile strength decreases with increasing W/T, although yield stress remains unaffected by changes in specimen width[7,36]. Decreasing W/T leads to increased post-necking elongation in structural steels due to variations in the necking behavior that changes from localized to diffuse necking, resulting in increased overall total elongation[37–40].

Specimen gauge length significantly impacts ductility measurements, where shorter gauge lengths lead to increases in post-necking elongation and total elongation[41–43]. A critical value based on the ratio of the original gauge length to the square root of the cross-sectional area $L_0/\sqrt{A}$ of 5.65 is typically adopted[7]. The amount of elongation that occurs during post-necking deformation is not influenced by gauge length, therefore uniform elongation is unaffected by gauge length.

The impact of specimen diameter and gauge length on material properties for round sub-sized specimens is similar to the impact of thickness and gauge length for flat sub-sized specimens[44]. That is, the diameter must contain a critical number of grains to accurately represent bulk properties, where critical values of the diameter-to-grain size ratio D/GS from 6 to 10 are typically adopted. Similarly to flat specimens, gauge length affects the ductility of the material. For instance, Yuan *et al.*[45] reported that reductions in the gauge length-to-diameter ratio L_0/D in pure copper increased post-necking and total elongation, while uniform elongation remained consistent regardless of specimen size.

The critical values for the specimen size effect based on the important ratios of sub-sized specimens and the impacted tensile properties are summarized in Table 1.

Sub-sized specimen design. Unlike the design of conventional standard-size specimens that are based on standards by ASTM (American Society for Testing and Materials), ISO (International Standards Organization), JIS (Japanese Industrial Standards), and related standardization organizations which provide strict specifications for the specimen dimensions and aspect ratios, currently standards for the design of sub-sized specimens are not available. The need for standardized design methodology has been widely acknowledged, and there are undergoing efforts in standard development by several organizations. Also, multiple MTT studies provide guidelines and recommendations for the design of sub-sized specimens[5].

Specimen Geometry Type	Specimen Dimensions Ratio	Critical Value	Impacted Tensile Properties
Flat	Thickness-to-Grain Size (T/GS)	6–10	YS, UTS, UE, PE, TE
Round	Diameter-to-Grain Size (D/GS)		
Flat	Width-to-Thickness (W/T)	5	UTS, PE, TE
Flat	Length-to-Square Root of Area ($L_0/\sqrt{A}$)	5.65	PE, TE
Round			

Table 1. Critical values for sub-sized specimen dimensions and impacted tensile properties.

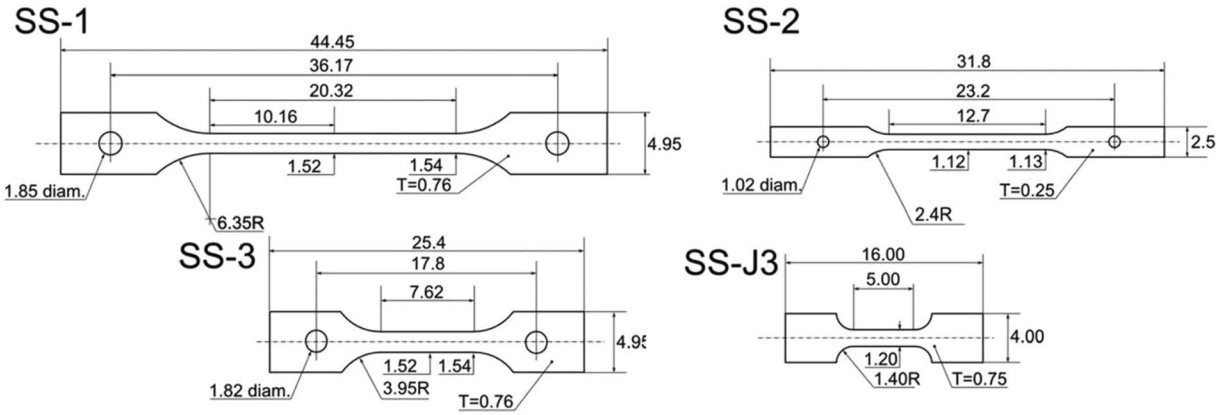

Fig. 3 Geometry and dimensions of sub-sized specimens from the SS and SS-J series. All dimensions are in millimeters. T denotes thickness. (Reprinted, with permission from[49]. Copyright ASTM International, http://www.astm.org).

MTT guidelines for the design of sub-sized specimens are summarized as follows[7,26,46,47]. (a) The specimen should at least have 6 to 10 grains in either thickness or diameter to represent the bulk material properties. (b) The specimen geometry should satisfy requirements for the aspect ratios W/T and $L_0/\sqrt{A}$ in order for the test results to be consistent with the standard-size specimens. (c) The design of the specimen should aim to reduce data variability, as sub-sized specimens often exhibit greater variability in test results compared to standard-sized specimens. (d) The volume of the specimens should be kept to a minimum to decrease the radioactivity of irradiated materials and mitigate risks during sample collection. (e) Specimen manufacturing costs should be considered in the design, e.g., flat sub-sized specimens are preferred because they are easier to manufacture compared to round specimens. (f) Testing and measurement equipment should be considered to ensure that the specimen design is a suitable fit for the available equipment.

Many different designs of sub-sized specimens presently exist, due to the lack of standardization. In general, the specimen design is typically either based on direct scaling of the dimensions of standard-sized specimens, or indirect scaling by applying additional adjustments to certain dimensions. The above requirements for lower bounding the minimal dimensions and other guidelines need to be observed in both cases. The former approach results in sub-sized specimens that have proportional geometry to dog-bone shaped standard-size specimens. The tensile properties of such specimens are often reported to be consistent with standard-sized specimens, although the size effect requires cautiousness and validation. In addition, proportional specimens may still have relatively large gauge lengths in comparison to the other dimensions. Further reduction in the specimen volume resulting in lower irradiation dose in the nuclear industry can be achieved by the latter approach, in which sub-sized specimens are designed with geometry that is not proportional to the standard-size specimens. Data analysis methods based on elongation conversion methods or inverse FEM have been used by researchers in designing the specimen geometry[48]. In most cases, these specimen designs include reduced gauge length, and are hence more suitable for tests in constrained irradiation facilities. Due to the specimen size effect, such design requires a more rigorous validation step, that is typically material dependent.

Examples of sub-sized specimens from the SS and SS-J series are shown in Fig. 3[49]. SS-1 specimen design was developed for the material science irradiation program in the Experimental Breeder Reactor-II reactor in the 1980s[50]. SS-2 design with smaller dimensions was subsequently developed to reduce the volume for irradiation tests[51]. SS-3 and SS-J3 designs with reduced gauge lengths of 7.62 mm and 5 mm, respectively, were developed in the 1990s for irradiation in the fast flux test facility[49]. Sub-sized specimens with gauge lengths as low as 2 mm have also been proposed for fitting into constrained irradiation volume and with reduced radiation dose[52].

Besides the dog-bone shape sub-sized specimens, other proposed shapes include bow-tie shape[53] and dumb-bell shape[54]. These specimens can address some of the challenges in tensile testing of miniature specimens, such as gripping of the specimen. On the other hand, these designs require specialized testing equipment and processing techniques, there is a small amount of tensile data available, and demand careful validation across different materials. Due to these reasons, dog-bone shape sub-sized specimens are still the norm in tensile testing.

Number of Records	Material Tested	Data Source	Dataset
17	SS304L, FeCrAl, A-718, Al-6061	Gussev *et al.*[5]	Byun *et al.*[60]
4	Zircaloy-4	Pierron *et al.*[61]	Experimental data
36	SS316L, F82H, SA-533	Gussev *et al.*[49]	Experimental data
421	JPCA, JFMS	Kohno *et al.*[36]	Experimental data
24	SS304, S235, S355	Rund *et al.*[33]	Experimental data
11	SA-508	Byun *et al.*[60]	Experimental data
2	Ultra-fine grain low carbon steel	Alsabbagh *et al.*[62]	Experimental data
14	Experimental low-carbon steel, Ti6Al4V, X14CrMoVNbN10, P91, EN AW, 6005 T6 Copper 99.99%	Džugan *et al.*[63]	Experimental data
8	Ti6Al4V	Van Zyl *et al.*[59]	Experimental data
25	DP600, DP800, SS316L	Zhang *et al.*[13]	Experimental data
26	20MnMoNi55, CrMoV, SS304LN	Kumar *et al.*[64]	Experimental data
22	Zircaloy-2, Zr-2.5 Nb	Balakrishnan *et al.*[65]	Experimental data
9	DC01	Konopík *et al.*[66]	Experimental data
3	CP AL (AL-99.6 wt.%)	Lanjewar *et al.*[67]	Experimental data
4	UNS S31035, Sanicro 25	Dymáček *et al.*[54]	Experimental data
3	Ti6Al4V	Sikan *et al.*[68]	Experimental data
72	SS316	Klueh[50]	Experimental data
40	SS304, SS316	Igata *et al.*[69]	Kestenbach *et al.*[70]
5	SS316L	Roach *et al.*[71]	Experimental data
238	SS316	Miyahara *et al.*[72]	Experimental data
22	SA-508	Yin *et al.*[73]	Experimental data
4	SS316	Do Kweon *et al.*[56]	Experimental data
4	SS316	Mishra *et al.*[74]	[75–86]
24	SS304, SS304L, SS316L	Seo *et al.*[57]	Experimental data

Table 2. Acquired number of data records and material type in the dataset per reference.

Data acquisition. The data was collected through a comprehensive search process of relevant scientific articles in the published literature. The search strategy was based on using various combinations of the following query terms: "tensile test," "sub-sized specimen," "mini specimen," "miniature specimen," "small specimen," "size effect," "stainless steel 316," "SS316," "reactor pressure vessel steel," "zirconium alloy," and "zircaloy." The quotation marks for the above terms indicate that the search queries comprised more than a single individual keyword. We used the Google Scholar website search engine, Google Chrome web browser search engine, and Microsoft Edge web browser search engine. Based on an extensive literature search using the listed specific terms, we identified 72 scientific peer-reviewed articles in total containing potentially relevant data for the task at hand.

In the next step, we applied three inclusion criteria to the retrieved articles for further refining the search process and identifying articles that contain relevant data. Inclusion criteria involved: (a) the article provides quantitative results of tensile tests with sub-sized specimens regarding yield strength, ultimate tensile strength, ultimate elongation, and total elongation; (b) the article provides information regarding the dimensions and geometry of used sub-sized specimens; and (c) the specimen material beongs to the following groups of nuclear structural materials: stainless steel (SS) 316 (grades SS316, SS316L, SS316LN, and SS316H), reactor pressure vessel steels (such as SA-508, SA-533, 20MnMoNi55), and fuel cladding Zirconium alloys (Zircaloy-2, Zircaloy-4, and Zr2.5 Nb). Articles lacking detailed experimental tensile test data, not employing sub-sized specimens, or focusing on different materials were excluded from the data extraction. This step resulted in 24 identified articles, listed in Table 2.

For the articles that provide structured tabular data of tensile test results and information related to specimen size, manufacturing treatment, and other relevant data in the form of tables, spreadsheets, or databases, we manually extracted the data and stored them in an Excel workbook. For the articles where the data appear solely in graphical form, we employed the plot digitization software WebPlotDigitizer[55] to manually extract the data for each point in the graphs. Examples include graphs of the distribution of the tensile properties as a function of the specimen dimensions. Material science experts double-checked the extracted tabular and graphical data to validate the accuracy and reduce the likelihood of human error. The total number of extracted tensile test records is 1,050. The number of records, material type, and the articles from which they are extracted are presented in Table 2.

Data post-processing. We applied several post-processing steps to ensure that all records in the dataset provide consistent information. Specifically, the extracted data from various articles contained information reported in different measurement units, such as testing or treatment temperatures reported in Celsius, Fahrenheit, and Kelvin degrees. We applied unit conversion for several features in the collected dataset to ensure consistency in the data records. Other similar examples include converting the strain-rate information for the tensile test from

Sub-sized Specimen Type	Gauge Length (mm)	Width (mm) or Diameter (mm)	Thickness (mm) or Diameter (mm)	Specimen Geometry	Number of Records
SS Mini 1S1, SS Mini 1E1[5]	2.55	0.8	0.4	Flat	2
SS Mini 1S2, SS Mini 1E2[5]	2.55	0.8	0.6	Flat	2
SS Mini 2S1, SS Mini 2E1[5]	3.55	0.8	0.4	Flat	6
SS Mini 2S2, SS Mini 2E2[5]	3.55	0.8	0.6	Flat	2
SS-1[49]	20.32	1.54	0.76	Flat	6
SS-2[49]	12.7	1.13	0.25	Flat	6
SS-3[49]	7.62	1.54	0.76	Flat	6
SS-J, SS-J3[5,49]	5	1.2	0.75	Flat	11
SS-Mini[49]	2.3	0.4	0.25	Flat	6
Rund *et al.*[33]	15	5	0.5	Flat	12
Džugan *et al.*[63]	3	1.5	0.5	Flat	19
Byun *et al.*[60]	10	3	[0.12:2]	Flat	11
Alsabbagh *et al.*[62]	2	0.2	1	Flat	2
Džugan *et al.*[63]	10	[4.84, 30, 7.99, 9.88, 5.01]	[4.84, 30, 7.99, 9.88, 5.01]	Round	7
Van Zyl *et al.*[59]	10	2	1	Flat	8
A80[13]	80	20	[1.2, 1.3, 1.6]	Flat	5
A50[13]	50	12.5	[1.2, 1.3, 1.6]	Flat	5
ASTM25[13]	25	6	[1.2, 1.3, 1.6]	Flat	5
Mini1[13]	10	3	[1.2, 1.3, 1.6]	Flat	5
Mini2[13]	5	2	[1.2, 1.3, 1.6]	Flat	5
Type I[64]	30	6	6	Round	13
Type II[64]	9.5	3	1	Flat	6
Type III[64]	3	1	0.3	Flat	13
Balakrishnan *et al.*[65]	[8.6 22]	[1.3 6]	[2.4 3.6, 4.3]	Flat	22
Konopík *et al.*[66]	[4 50]	[1 1.5]	[0.2 0.5 1.5]	Flat	12
Lanjewar *et al.*[67]	3	1	1.3	Flat	3
Dymáček *et al.*[54]	4	2	1	Flat	2
Dymáček *et al.*[54], Do Kweon[56], Mishra *et al.*[74]	25	5	5	Round	28
Sikan *et al.*[68]	3	1	0.5	Flat	3
Klueh[50]	[7.62 12.7 20.32]	[1.02 1.52]	[0.25 0.76]	Flat	54
Klueh[50]	18.3	2.03	2.03	Round	18
Igata *et al.*[69]	[15 30]	4	[0.0032 0.1 0.185 0.2 0.35]	Flat	39
Roach *et al.*[71]	[1.6, 2.4, 4, 10, 25]	[0.4, 0.6, 1.0, 2.5, 6.25]	[0.4, 0.6, 1.0, 2.5, 6.25]	Round	5
Yin *et al.*[73]	[6, 10, 15]	[3.2, 4, 6.4]	[0.5, 1, 2]	Flat	22
Do Kweon[56]	25	6	6	Round	2
Miyahara *et al.*[72]	15	4	[0.02, 0.1, 0.15, 0.2, 0.3, 0.35, 0.5]	Flat	238
ASTM 1:1[61]	10	10	0.64	Flat	1
ASTM 3:2 A[61]	15	10	0.64	Flat	1
ASTM 3:2B[61]	15	10	0.64	Flat	1
ASTM 4:1[61]	40	10	0.64	Flat	1
ASTM A[49]	28	6	6	Flat	6
Kohno *et al.*[36]	5	1.2	[0.06, 1.03]	Flat	421
Seo *et al.*[57]	[5, 20, 38]	[3, 5]	[3, 5]	Round	17

Table 3. Dimensions of sub-sized specimens in the dataset. Note: the brackets in some of the fields indicate that multiple values are used for that specimen dimension in the corresponding reference.

strain/minutes to strain/seconds, as well as cases where the articles only disclosed the used machine speed and we derived the strain rate based on the sample length and machine speed. Strain rate sensitivity is an important factor that can influence the tensile test results, as prior works report increased yield strength and ultimate tensile strength with increased strain rate[13,33,56,57]. Furthermore, the information for the material composition in several papers included the term "balance" to indicate that the remainder of the composition is made up of the specified primary element providing the base structure after accounting for all other elements (e.g., Iron (Fe) in SS316). We calculated the composition of the primary element to ensure that the weight percentage of all elements in the provided composition data sums to 100%, and we replaced the term "balance" with the calculated value. We confirmed the accuracy of the composition for each record in the dataset by ensuring that the sum of the elements is consistently 100% with no outliers.

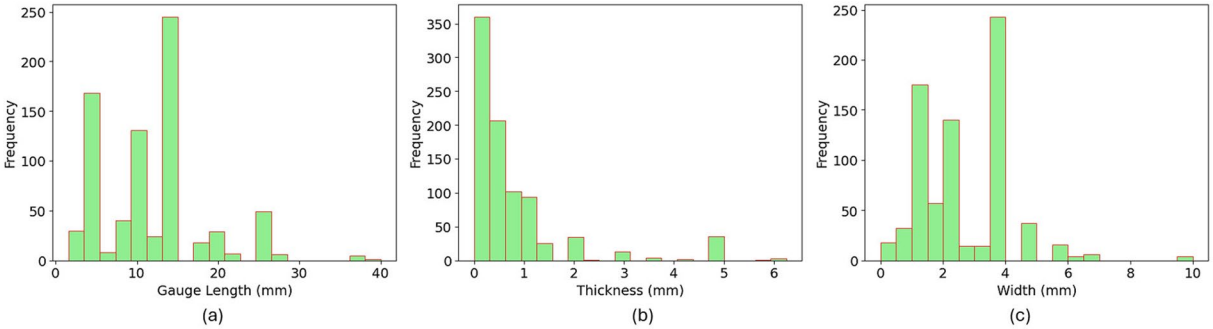

Fig. 4 Histograms for the dimensions of sub-sized specimens: (**a**) gauge length, (**b**) width or diameter, (**c**) thickness or diameter.

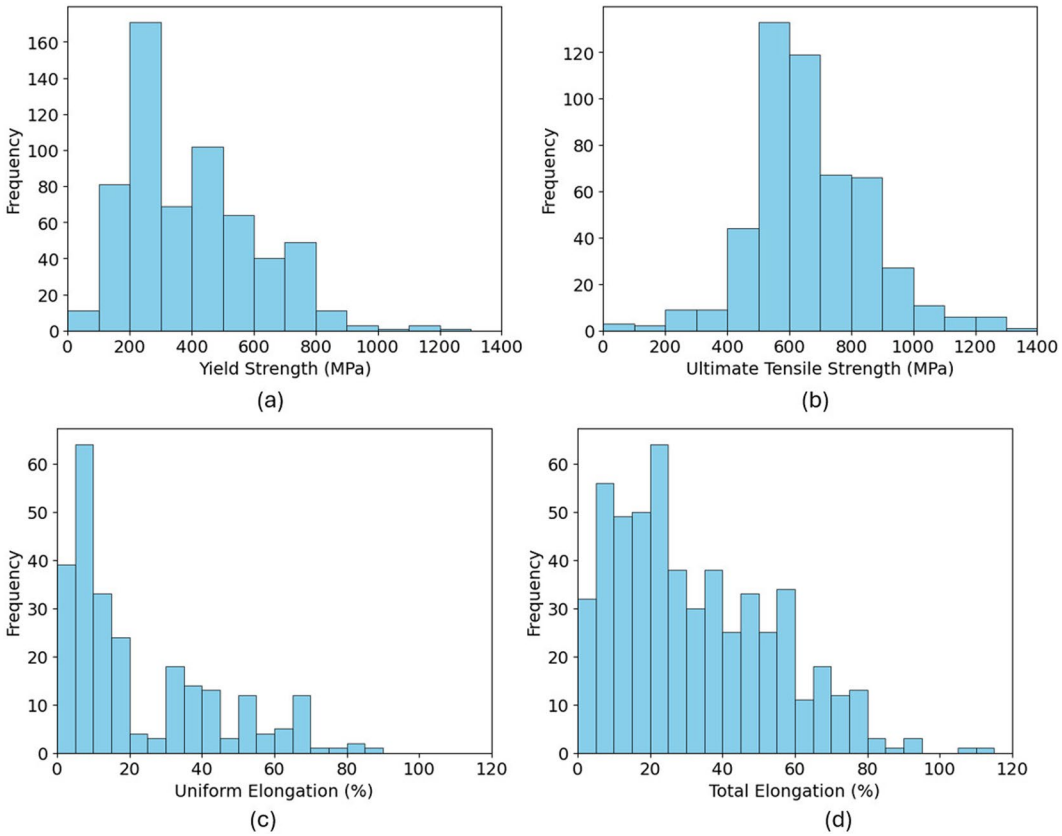

Fig. 5 Histograms of tensile test properties: (**a**) yield strength, (**b**) ultimate tensile strength, (**c**) uniform elongation, and (**d**) total elongation.

Specimen size. The dimensional information of the sub-sized specimens in the dataset, related to the gauge length, width or diameter, and thickness or diameter, along with the specimen geometry and number of records in the dataset is presented in Table 3. Histograms of the distribution of gauge length, width, and thickness for the specimens in the dataset are shown in Fig. 4.

Tensile properties. The collected data for the tensile properties encompass information for yield strength, ultimate tensile strength, uniform elongation, and total elongation. The units for yield strength and ultimate tensile strength are MPa (Mega Pascals), and percent (%) for elongation. The distributions of the tensile properties for the sub-sized specimens in the dataset are shown in the histograms in Fig. 5.

Manufacturing treatment and irradiation conditions. Manufacturing treatment of tensile test specimens and irradiation conditions are among the most important factors that affect tensile test results. The differences in processing, such as cold work, heat treatment and irradiation, can significantly affect material microstructure such as dislocation density, grain size and precipitate size, and therefore impact tensile properties like strength

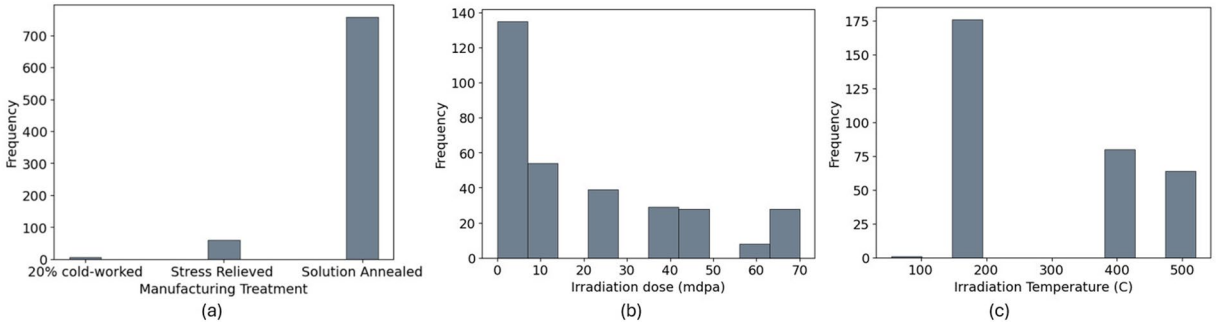

Fig. 6 Histograms of (**a**) manufacturing treatment (**b**) irradiation dose, and (**c**) irradiation temperature.

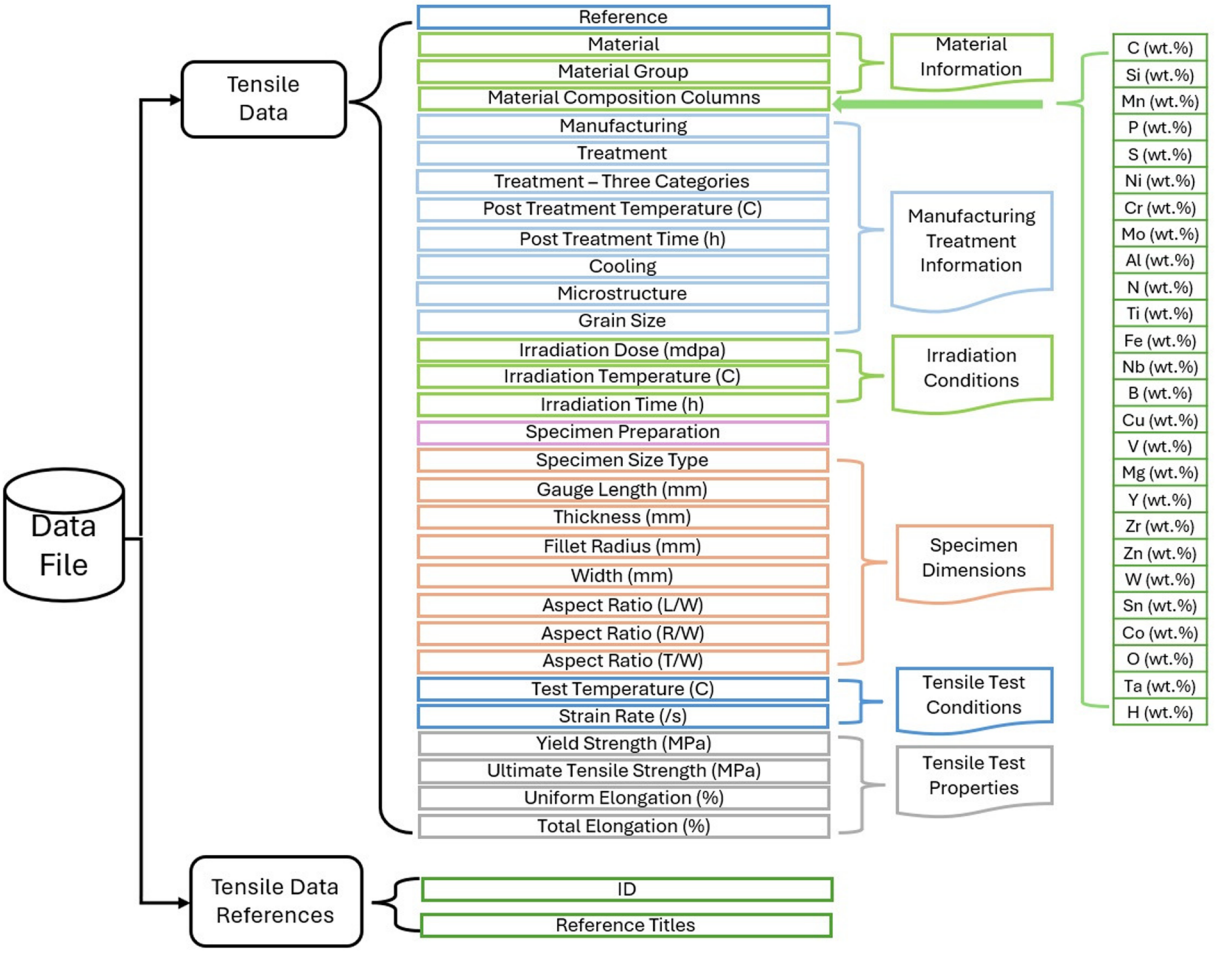

Fig. 7 Organization of the dataset by columns and data categories.

and ductility. Proper specimen preparation is essential for obtaining reliable tensile properties, as any variation in surface quality, shape, or machining precision can significantly alter the material's performance during testing. Additionally, test conditions such as strain rate sensitivity can influence tensile test results, as prior works reported increased yield strength and ultimate tensile strength with increased strain rate[13,33,56,57].

Histograms of the distribution of manufacturing treatment of the specimens and irradiation conditions related to the irradiation dose and temperature are presented in Fig. 6.

Data Records

The dataset is available at the Materials Cloud Archive[58]. The extracted data are stored in a Microsoft Excel workbook format. The structure of the dataset is schematically depicted in Fig. 7. Each row corresponds to retrieved information for a single tensile test. The information for each record consists of 55 columns, divided into the following categories: Reference, Material Type and Composition, Manufacturing and Treatment

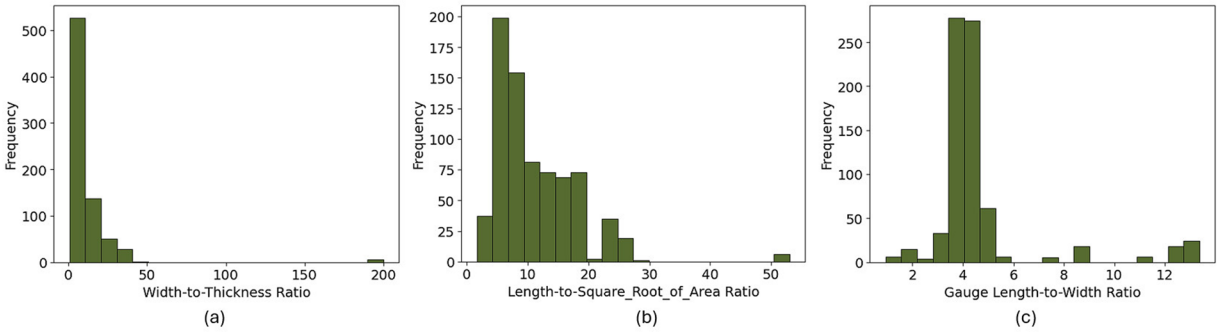

Fig. 8 Histograms of aspect ratios for the sub-sized specimens in the dataset: (**a**) width-to-thickness ratio, (**b**) length-to-square-root-of-area ratio, (**c**) gauge length-to-width ratio.

Information, Irradiation Conditions, Specimen Preparation, Specimen Dimensions, Tensile Test Conditions, and Tensile Properties. The columns in the Reference category list the article from which the data were extracted. The Material Type and Composition columns record the material type of the sub-specimens and their chemical composition listing the elements given in weight percentage. The category Manufacturing and Treatment Information documents the type of treatment, post-treatment temperature (°C) and time (hours), microstructure, morphology, grain size (μm), and similar information. The Irradiation Conditions columns, if applicable to the tensile test record, provide information regarding the irradiation dose (milli-displacement per atom), temperature (°C), and time (hours). The information for all columns in the Manufacturing and Treatment Information and Irradiation Conditions were not provided in all articles, and as a result, some test records have missing information (e.g., for microstructure, or grain size). Specimen Preparation is providing the machining techniques and surface finishing methods, such as grinding and polishing with mechanical, chemical, and electrolytic techniques. Specimen Dimensions are provided in millimeters and present information regarding the gauge length, width, thickness, fillet radius, and aspect ratios of the dimensions of sub-sized specimens. Tensile Test Conditions provide information regarding the temperature of the tensile test (°C), and the strain rate ($1/s$) of the test. Finally, Tensile Properties include data on yield strength (MPa), ultimate tensile strength (MPa), uniform elongation (%), and total elongation (%). Each category label is color-coded in the Excel workbook.

Besides the main worksheet containing the data, the Excel workbook contains a worksheet References that lists the papers from which the data was extracted, and a worksheet Column Descriptions that provides descriptions of the columns in the dataset.

Technical Validation

To ensure data validity, materials science experts conducted a thorough review of all retrieved data from the literature. This step involved ensuring the accuracy of the material type and use of standardized material names and verifying the chemical composition of the materials in the dataset. The experts validated the information for the manufacturing processes and treatment methods, testing conditions, specimen size, and tensile test properties. Similarly, the conversion of extracted information to consistent units was validated. Furthermore, our team of experts performed statistical analyses and applied data visualization techniques to identify and address data outliers, ensuring the reliability of the dataset.

We analyzed the data to validate the MTT recommendations for sub-sized specimens to ensure that the material bulk properties are maintained and that analytical data techniques can be applied to account for the specimen size effect. Most sub-sized specimens selected for this dataset have thickness of 0.2 mm or greater (to ensure containing at least 10 grains)[7], however we elected to include data from several thinner specimens with thicknesses of: 0.02, 0.1, 0.06, and 0.15 mm. It is important to note that these thickness values are part of a study where the authors varied the thickness of the specimen to evaluate the impact on tensile properties[59], and are not actual specimen designs used in practice. We didn't discard these data points although they violate the recommendations for minimum thickness, because we believe that keeping the data can be helpful for studies of the specimen size effect. As stated earlier, recommendations for the ratio of width-to-thickness W/T are to not be lower than a critical value of around 5. The histogram of the width-to-thickness ratio is shown in Fig. 8(a). Similarly, for the ratio of the gauge length to the square root of the cross-sectional area $L_0/\sqrt{A}$, the recommended critical value is 5.65. The histogram of the $L_0/\sqrt{A}$ ratio is plotted in Fig. 8(b), showing that 79% of the records have the recommended aspect ratio. The recommended values for the length-to-width ratio L_0/W for sub-sized specimens are typically in the range from 3 to 6, with most specimen designs having a value of approximately 4[7]. Based on the histogram of the L_0/W ratio shown in Fig. 8(c), 87% of the data records fall within that range. Some specimen geometries (such as SS-1 and SS-2) have a length-to-width ratio over 10, whereas some other designs (such as ASTM 1:1 and ASTM 3:2) have smaller aspect ratios of 2 and below. We retained these data records, because they represent valid sub-sized specimen designs, and they can benefit studies of the specimen size effect.

Code availability

Sample code in Python and Jupyter Notebooks for loading the dataset and analysis of the results are available at the following link: https://github.com/avakanski/Subsized-Specimens-Tensile-Properties/blob/main/Sample_Code.ipynb.

Received: 3 July 2024; Accepted: 18 December 2024;
Published online: 11 January 2025

References

1. Ramana, M. V. Small modular and advanced nuclear reactors: A reality check. *IEEE Access* **9**, 42090–42099, https://doi.org/10.1109/ACCESS.2021.3064948 (2021).
2. Stacey, W. M. *Nuclear Reactor Physics*. https://www.wiley.com/en-us/Nuclear+Reactor+Physics (John Wiley & Sons, 2018).
3. Li, G. *et al*. Modeling and control of nuclear reactor cores for electricity generation: A review of advanced technologies. *Renew. Sustain. Energy Rev.* **60**, 116–128, https://doi.org/10.1016/j.rser.2016.01.116 (2016).
4. Olson, G. B. & Kuehmann, C. J. Materials genomics: From CALPHAD to flight. *Scripta Mater.* **70**, 25–30, https://doi.org/10.1016/j.scriptamat.2013.08.032 (2014).
5. Gussev, M. N., Howard, R. H., Terrani, K. A. & Field, K. G. Sub-size tensile specimen design for in-reactor irradiation and post-irradiation testing. *Nucl. Eng. Des.* **320**, 298–308, https://doi.org/10.1016/j.nucengdes.2017.06.008 (2017).
6. Hosemann, P., Shin, C. & Kiener, D. Small scale mechanical testing of irradiated materials. *J. Mater. Res.* **30**, 1231–1245, https://doi.org/10.1557/jmr.2015.26 (2015).
7. Zheng, P. *et al*. On the standards and practices for miniaturized tensile test–A review. *Fusion Eng. Des.* **161**, 112006, https://doi.org/10.1016/j.fusengdes.2020.112006 (2020).
8. Prasitthipayong, A. *et al*. Micro mechanical testing of candidate structural alloys for Gen-IV nuclear reactors. *Nucl. Mater. Energy* **16**, 34–45, https://doi.org/10.1016/j.nme.2018.05.018 (2018).
9. Reer, J. R., Jang, D. & Gu, X. W. Exploring deformation mechanisms in nanostructured materials. *JOM* **64**, 1241–1252, https://doi.org/10.1007/s11837-012-0438-6 (2012).
10. Hurst, R.C. & Matocha, K. A renaissance in the use of the small punch testing technique. *In Pressure Vessels and Piping Conference*, **56932**, V01BT01A048. American Society of Mechanical Engineers, West Conshohocken, PA https://doi.org/10.1115/PVP2015-45095 (2015).
11. Suzuki, K., Jitsukawa, S., Okubo, N. & Takada, F. Intensely irradiated steel components: Plastic and fracture properties, and a new concept of structural design criteria for assuring the structural integrity. *Nucl. Eng. Des.* **240**, 1290–1305, https://doi.org/10.1016/j.nucengdes.2010.02.031 (2010).
12. Tomaszewski, T. Statistical Size Effect in Fatigue Properties for Mini-Specimens. *Materials* **13**, 2384, https://doi.org/10.3390/ma13102384 (2020).
13. Zhang, L., Harrison, W., Yar, M., Brown, S. & Lavery, N. The development of miniature tensile specimens with non-standard aspect and slimness ratios for rapid alloy prototyping processes. *J. Mater. Res. Technol.* **15**, 1830–1843, https://doi.org/10.1016/j.jmrt.2021.09.029 (2021).
14. International Organization for Standardization. Steel-Conversion of Elongation Values-Part 1: Carbon and Low Alloy Steels. ISO 2566-1, https://www.iso.org/standard/7524.html (1984).
15. Dieter, G. E. Mechanical Metallurgy. 3rd ed. https://books.google.com/books/Mechanical_Metallurgy (McGraw-Hill, 1986).
16. Hyun, H. C., Kim, M., Bang, S. & Lee, H. On acquiring true stress–strain curves for sheet specimens using tensile test and FE analysis based on a local necking criterion. *J. Mater. Res.* **29**, 695–707, https://doi.org/10.1557/jmr.2014.24 (2014).
17. Clyne, T. W., Campbell, J. E., Burley, M. & Dean, J. Profilometry-based inverse finite element method indentation plastometry. *Adv. Eng. Mater.* **23**, 2100437, https://doi.org/10.1002/adem.202100437 (2021).
18. Kamaya, M., Kitsunai, Y. & Koshiishi, M. True stress–strain curve acquisition for irradiated stainless steel including the range exceeding necking strain. *J. Nucl. Mater.* **465**, 316–325, https://doi.org/10.1016/j.jnucmat.2015.05.027 (2015).
19. Oliver, D. Proposed new criteria of ductility from a new law connecting the percentage elongation with size of test-piece. *Proc. Inst. Mech. Eng.* **115**, 827–864, https://doi.org/10.1243/PIME_PROC_1928_115_019_02 (1928).
20. Wallin, K., Karjalainen-Roikonen, P. & Suikkanen, P. Sub-sized CVN specimen conversion methodology. *Procedia Struct. Integr.* **2**, 3735–3742, https://doi.org/10.1016/j.prostr.2016.06.464 (2016).
21. Biswas, S., Fernandez Castellanos, D. & Zaiser, M. Prediction of creep failure time using machine learning. *Sci. Rep.* **10**, 16910, https://doi.org/10.48550/arXiv.2005.03514 (2020).
22. Li, L. *et al*. Uncertainty quantification in multivariable regression for material property prediction with Bayesian neural networks. *Scien. Reports.* **14**(10543), 1–15, https://doi.org/10.48550/arXiv.2311.02495 (2024).
23. Boehnlein, A. *et al*. Colloquium: Machine learning in nuclear physics. *Rev. Mod. Phys.* **94**, 031003, https://doi.org/10.48550/arXiv.2112.02309 (2022).
24. Agrawal, A. & Choudhary, A. Perspective: materials informatics and big data: realization of the 'fourth paradigm' of science in materials science. *APL Mater* **4**, 053208, https://doi.org/10.1063/1.4946894 (2016).
25. Schwab, K. The Fourth Industrial Revolution. *Foreign Aff* **95**, 3–7, https://www.foreignaffairs.com/world/fourth-industrial-revolution (2016).
26. Lucon, E. Testing of small-sized specimens. In: *Comprehensive Materials Processing*, Elsevier, Amsterdam, **1**, https://doi.org/10.1016/B978-0-08-096532-1.00110-2 (2014).
27. Arbeiter, F. *et al*. The accomplishments of lithium target and test facility validation activities in the IFMIF/EVEDA phase. *Nucl. Fusion* **58**(1), 015001, https://doi.org/10.1088/1741-4326/aa8ba5 (2018).
28. Wakai, E. *et al*. Small specimen test technology development towards design of fusion DEMO reactors and future direction plan. *In: IAEA Fusion Energy Conference*, Kyoto, Japan, October 17-22, https://nucleus.iaea.org (2016).
29. Spearing, S. M. Materials issues in microelectromechanical systems (MEMS). *Acta Mater* **48**, 179–196, https://doi.org/10.1016/S1359-6454(99)00294-3 (2000).
30. Read, D. T. *et al*. Measuring flow curve and failure conditions for a MEMS-scale electrodeposited nickel alloy. *Mater. Res. Express* **6**, 0950a6, https://doi.org/10.1088/2053-1591/aae6ad (2019).
31. Gupta, S. *et al*. MEMS based nanomechanical testing method with independent electronic sensing of stress and strain. *Extreme Mech. Lett.* **8**, 167–176, https://doi.org/10.1016/j.eml.2016.01.005 (2016).
32. Sharpe, W. N. Jr, Yuan, B., Vaidyanathan, R. & Edwards, R. L. New test structures and techniques for measurement of mechanical properties of MEMS materials. In *Microlithogr. Metrology Micromach*. 2880, 78-91. SPIE, https://doi.org/10.1117/12.250969 (1996).
33. Rund, M., Procházka, R., Konopík, P., Džugan, J. & Folgar, H. Investigation of sample-size influence on tensile test results at different strain rates. *Procedia Eng* **114**, 410–415, https://doi.org/10.1016/j.proeng.2015.08.086 (2015).
34. Yang, L. & Lu, L. The influence of sample thickness on the tensile properties of pure Cu with different grain sizes. *Scripta Mater* **69**, 242–245, https://doi.org/10.1016/j.scriptamat.2013.04.009 (2013).

35. Chen, F. *et al*. Size effects on tensile strength of aluminum–bronze alloy at room temperature. *Mater. Des.* **85**, 778–784, https://doi.org/10.1016/j.matdes.2015.06.169 (2015).
36. Kohno, Y. *et al*. Specimen size effects on the tensile properties of JPCA and JFMS. *J. Nucl. Mater.* **283-287**, 1014–1017, https://doi.org/10.1016/S0022-3115(00)00245-2 (2000).
37. Mikkelsen, L. P. Necking in rectangular tensile bars approximated by a 2-D gradient-dependent plasticity model. *Eur. J. Mech. A/Solids* **18**, 805–818, https://doi.org/10.1016/S0997-7538(99)00113-8 (1999).
38. Zhang, Z. L., Hauge, M., Ødegård, J. & Thaulow, C. Determining material true stress–strain curve from tensile specimens with rectangular cross-section. *Int. J. Solids Struct.* **36**, 3497–3516, https://doi.org/10.1016/S0020-7683(98)00153-X (1999).
39. Zhao, Y. H. *et al*. Influence of specimen dimensions and strain measurement methods on tensile stress–strain curves. *Mater. Sci. Eng. A* **525**, 68–77, https://doi.org/10.1016/j.msea.2009.06.031 (2009).
40. Brooks, I., Palumbo, G., Hibbard, G. D., Wang, Z. & Erb, U. On the intrinsic ductility of electrodeposited nanocrystalline metals. *J. Mater. Sci.* **46**, 7713–7724, https://doi.org/10.1007/s10853-011-5751-x (2011).
41. Lord, J. D., Roebuck, B., Morrell, R. & Lube, T. 25 year perspective: Aspects of strain and strength measurement in miniaturised testing for engineering metals and ceramics. *Mater. Sci. Technol.* **26**, 127–148, https://doi.org/10.1179/026708309X12584564052012 (2010).
42. Strnadel, B. & Brumek, J. The size effect in tensile test of steels. In: ASME 2013 Pressure -tVessels and Piping Conference, 55713, V06BT06A058 https://doi.org/10.1115/PVP2013-98162 (2013).
43. Zhao, Y. H. *et al*. Influence of specimen dimensions on the tensile behavior of ultrafine-grained Cu. *Scr. Mater.* **59**, 627–630, https://doi.org/10.1016/j.scriptamat.2008.05.031 (2008).
44. Hyde, T. H., Sun, W. & Williams, J. A. Requirements for and use of miniature test specimens to provide mechanical and creep properties of materials: a review. *Int. Mater. Rev.* **52**, 213–255, https://doi.org/10.1179/174328007X160317 (2007).
45. Yuan, W. J. *et al*. An analysis on necking effect and stress distribution in round cross-section specimens of pure copper with different diameters. *Mater. Sci. Eng. A* **561**, 183–190, https://doi.org/10.1016/j.msea.2012.10.077 (2013).
46. Field, K. G., Gussev, M. N., Hu, X., Yamamoto, Y. & Howard, R. H. First annual progress report on radiation tolerance of controlled fusion welds in high temperature oxidation resistant FeCrAl alloys. *ORNL/TM-2015/770*, https://doi.org/10.2172/1235007 (2015).
47. Lucon, E., Bicego, V., D'Angelo, D. & Fossati, C. Evaluating a service-exposed component's mechanical properties by means of subsized and miniature specimens. *ASTM Spec. Tech. Publ.* **1204**, 311–311, https://doi.org/10.1520/STP12738S (1993).
48. Liu, H., Chen, R., Wen, M., Zhang, L. & Shen, Y. Optimizing parallel section length for small tensile specimen with fabrication non-uniformity in thickness. *Fusion Eng. Des.* **147**, 111244, https://doi.org/10.1016/j.fusengdes.2019.111244 (2019).
49. Gussev, M., Busby, J., Field, K., Sokolov, M. & Gray, S. Role of scale factor during tensile testing of small specimens. *Small Specimen Test Techniques*: **6**, 31–49, ed. M. Sokolov, E. Lucon https://doi.org/10.1520/STP157620140013 (2015).
50. Klueh, R. L. Miniature tensile test specimens for fusion reactor irradiation studies. *Nucl. Eng. Des. Fusion* **2**(3), 407–416, https://doi.org/10.1520/STP157620140013 (1985).
51. Bauer, R. E. Instrumented in-reactor test capabilities in FFTF. *J. Nucl. Mater.* **104**, 1563–1565, https://doi.org/10.1016/0022-3115(82)90823-6 (1981).
52. Liu, H., Shen, Y., Yang, S., Zheng, P. & Zhang, L. A comprehensive solution to miniaturized tensile testing: Specimen geometry optimization and extraction of constitutive behaviors using inverse FEM procedure. *Fusion Eng. Des.* **121**, 188–197, https://doi.org/10.1016/j.fusengdes.2017.07.016 (2017).
53. LaVan, D. & Sharpe, W. Tensile testing of microsamples. *Exp. Mech.* **39**, 210–216, https://link.springer.com/article/10.1007/BF02323554 (1999).
54. Dymáček, P., Jarý, M., Dobeš, F. & Kloc, L. Tensile and creep testing of Sanicro 25 using miniature specimens. *Materials* **11**, 142, https://doi.org/10.3390/ma11010142 (2018).
55. Automeris. *WebPlotDigitizer* https://apps.automeris.io/wpd4/ (2024).
56. Do Kweon, H., Kim, J. W., Song, O. & Oh, D. Determination of true stress-strain curve of type 304 and 316 stainless steels using a typical tensile test and finite element analysis. *Nucl. Eng. Technol.* **53**(2), 647–656, https://doi.org/10.1016/j.net.2020.07.014 (2021).
57. Seo, J.-M. *et al*. Modification of the Johnson–Cook model for the strain rate effect on tensile properties of 304/316 austenitic stainless steels. *J. Press. Vess. Technol.* **144**, 011501, https://doi.org/10.1115/1.4050833 (2022).
58. Li, L. *et al*. Dataset of tensile properties for sub-sized specimens of nuclear structural materials (Version v3) [Data set]. *Materials Cloud Archive* **2024.153**, https://doi.org/10.24435/materialscloud:ws-8j (2024).
59. Van Zyl, I., Moletsane, M., Yadroitsava, I., Yadroitsev, I. & Krakhmalev, P. Validation of miniaturised tensile testing on DMLS TI6Al4V (ELI) specimens. *S. Afr. J. Ind. Eng.* **27**(3), 192–200, https://doi.org/10.7166/27-3-1666 (2016).
60. Byun, T. S., Kim, J. H., Chi, S. H. & Hong, J. H. Effect of specimen thickness on the tensile deformation properties of SA508 Cl. 3 reactor pressure vessel steel. *Small Specimen Test Techniques*. https://doi.org/10.1520/STP38013S (1998).
61. Pierron, O. N., Koss, D. A. & Motta, A. T. Tensile specimen geometry and the constitutive behavior of Zircaloy-4. *J. Nucl. Mater.* **312**(2-3), 257–261, https://doi.org/10.1016/S0022-3115(02)01554-4 (2003).
62. Alsabbagh, A., Valiev, R. Z. & Murty, K. L. Influence of grain size on radiation effects in a low carbon steel. *J. Nucl. Mater.* **443**(1-3), 302–310, https://doi.org/10.1016/j.jnucmat.2013.07.049 (2013).
63. Džugan, J., Procházka, R. & Konopík, P. Micro-tensile test technique development and application to mechanical property determination. In *Small Specimen Test Techniques*: **6**, STP 1576. ASTM Int. https://doi.org/10.1520/STP157620140022 (2015).
64. Kumar, K. *et al*. Use of miniature tensile specimen for measurement of mechanical properties. *Procedia Eng* **86**, 899–909, https://doi.org/10.1016/j.proeng.2014.11.112 (2014).
65. Balakrishnan, K. S., Samal, M. K., Parashar, J., Tiwari, G. P. & Anatharaman, S. Suitability of miniature tensile specimens for estimating the mechanical property data of pressure tubes: an assessment. *Trans. Indian Inst. Met.* **67**, 47–55, https://doi.org/10.1007/s12666-013-0316-0 (2014).
66. Konopík, P., Farahnak, P., Rund, M., Džugan, J. & Rzepa, S. Applicability of miniature tensile test in the automotive sector. In *IOP Conf. Ser. Mater. Sci. Eng.* **461**(1), 012043, https://doi.org/10.1088/1757-899X/461/1/012043 (2018).
67. Lanjewar, H. A., Naghdy, S., Kestens, L. A. I. & Verleysen, P. Miniature tensile testing of SPD processed fine-grained aluminum. In *J. Phys. Conf. Ser.* **1270**(1), 012022, https://doi.org/10.1088/1742-6596/1270/1/012022 (2019).
68. Sikan, F., Wanjara, P., Gholipour, J. & Brochu, M. Use of miniature tensile specimens for measuring mechanical properties in the steady-state and transient zones of Ti–6Al–4V wire-fed electron beam deposits. *Mater. Sci. Eng.* **862**, 144487, https://doi.org/10.1016/j.msea.2022.144487 (2023).
69. Igata, N., Miyahara, K., Uda, T. & Asada, S. Effects of specimen thickness and grain size on the mechanical properties of types 304 and 316 austenitic stainless steel. In *The Use of Small-Scale Specimens for Testing Irradiated Material*, **STP 888**, ASTM Int. https://doi.org/10.1520/STP33000S (1986).
70. Kestenbach, H. J. & Meyers, M. A. The effect of grain size on the shock-loading response of 304-type stainless steel. *Metall. Trans. A* **7**, 1943–1950, https://doi.org/10.1007/BF02659827 (1976).
71. Roach, A. M. *et al*. Size-dependent stochastic tensile properties in additively manufactured 316L stainless steel. *Addit. Manuf.* **32**, 101090, https://doi.org/10.1016/j.addma.2020.101090 (2020).
72. Miyahara, K., Tada, C., Uda, T. & Igata, N. The effects of grain and specimen sizes on mechanical properties of type 316 austenitic stainless steel. *J. Nucl. Mater.* **133**, 506–510, https://doi.org/10.1016/0022-3115(85)90199-0 (1985).

73. Yin, S., Wang, X., Qiang, W., Qiao, J. & Wu, Y. Size effects on tensile properties of Chinese reactor pressure vessel steels and its semi-empirical normalization. *J. Nucl. Mater.* **579**, 154384, https://doi.org/10.1016/j.jnucmat.2023.154384 (2023).
74. Mishra, P. *et al*. Microstructural Characterization and Mechanical Properties of L-PBF Processed 316 L at Cryogenic Temperature. *Materials* **14**(19), 5856, https://doi.org/10.3390/ma14195856 (2021).
75. Casati, R., Lemke, J. & Vedani, M. Microstructure and fracture behavior of 316L austenitic stainless steel produced by selective laser melting. *J. Mater. Sci. Technol.* **32**, 738–744, https://doi.org/10.1016/j.jmst.2016.06.016 (2016).
76. Wang, Y. M. *et al*. Additively manufactured hierarchical stainless steels with high strength and ductility. *Nat. Mater.* **17**, 63–71, https://doi.org/10.1038/nmat5021 (2018).
77. Bidulský, R. *et al*. Case study of the tensile fracture investigation of additive manufactured austenitic stainless steels treated at cryogenic conditions. *Materials* **13**, 3328, https://doi.org/10.3390/ma13153328 (2020).
78. Suzuki, K., Fukakura, J. & Kashiwaya, H. Cryogenic fatigue properties of 304L and 316L stainless steels compared to mechanical strength and increasing magnetic permeability. *J. Test. Eval.* **16**, 190–197, https://doi.org/10.1520/JTE11161J (1988).
79. Lee, K. J., Chun, M. S., Kim, M. H. & Lee, J. M. A new constitutive model of austenitic stainless steel for cryogenic applications. *Comput. Mater. Sci.* **46**, 1152–1162, https://doi.org/10.1016/j.commatsci.2009.06.003 (2009).
80. Tolosa, I., Garciandía, F., Zubiri, F., Zapirain, F. & Esnaola, A. Study of mechanical properties of AISI 316 stainless steel processed by selective laser melting, following different manufacturing strategies. *Int. J. Adv. Manuf. Technol.* **51**, 639–647, https://doi.org/10.1007/s00170-010-2631-5 (2010).
81. Qiu, C., Al Kindi, M., Aladawi, A. S. & Al Hatmi, I. A comprehensive study on microstructure and tensile behaviour of a selectively laser melted stainless steel. *Sci. Rep.* **8**, 7785, https://doi.org/10.1038/s41598-018-26136-7 (2018).
82. Zhong, Y., Liu, L., Wikman, S., Cui, D. & Shen, Z. Intragranular cellular segregation network structure strengthening 316L stainless steel prepared by selective laser melting. *J. Nucl. Mater.* **470**, 170–178, https://doi.org/10.1016/j.jnucmat.2015.12.034 (2016).
83. Saeidi, K., Kvetková, L., Lofaj, F. & Shen, Z. Austenitic stainless steel strengthened by the *in situ* formation of oxide nanoinclusions. *RSC Adv* **5**, 20747–20750, https://doi.org/10.1039/c4ra16721j (2015).
84. Mower, T. M. & Long, M. J. Mechanical behavior of additive manufactured, powder-bed laser-fused materials. *Mater. Sci. Eng. A* **651**, 198–213, https://doi.org/10.1016/j.msea.2015.10.068 (2016).
85. ASTM Committee F42 on Additive Manufacturing Technologies, Subcommittee F42.91 on Terminology. *Standard Terminology for Additive Manufacturing Technologies*. ASTM International, West Conshohocken, PA, USA. https://www.astm.org/get-involved/technical-committees/committee-f42/subcommittee-f42 (2012).
86. Brnic, J., Niu, J., Canadija, M., Turkalj, G. & Lanc, D. Behavior of AISI 316L steel subjected to uniaxial state of stress at elevated temperatures. *J. Mater. Sci. Technol.* **25**, 175 https://www.jmst.org/EN/Y2009/V25/I02/175 (2009).

Acknowledgements

This work was supported through the INL Laboratory Directed Research& Development (LDRD) Program under DOE Idaho Operations Office Contract DE-AC07-05ID14517 (project tracking number 24A1081-149). Accordingly, the publisher, by accepting the article for publication, acknowledges that the U.S. Government retains a nonexclusive, paid-up, irrevocable, worldwide license to publish or reproduce the published form of this manuscript or allow others to do so, for U.S. Government purposes.

Author contributions

F.X., J.M., and R.S. developed the concept for the study. L.L., Y.T., F.X., and A.V. conducted the literature search and extracted the data. R.S. and J.R. analysed the data and contributed to the data validation. L.L., A.V., and F.X. drafted the first version of the manuscript. All authors reviewed the manuscript.

Competing interests

The authors declare no competing interests.

Additional information

Correspondence and requests for materials should be addressed to A.V. or F.X.

Reprints and permissions information is available at www.nature.com/reprints.

Publisher's note Springer Nature remains neutral with regard to jurisdictional claims in published maps and institutional affiliations.